Coherence properties of a quasi-Gaussian submilliradiant divergence soft-x-ray laser pumped by capillary discharges

A. Ritucci,[1] G. Tomassetti,[1] A. Reale,[1] F. Flora,[2] and L. Mezi[2]
[1]*Department of Physics, University of L'Aquila, gc LNGS of INFN, 67010 Coppito, L'Aquila, Italy*
[2]*ENEA Dipartimento Innovovazione, Divisione Fisica Applicata, CRE Frascati, Cassella Postale 65, 00044, Italy*
(Received 5 March 2004; published 27 August 2004)

The coherence properties of a 46.9-nm soft-x-ray laser beam produced in a capillary discharge plasma have been investigated. The beam is produced in a regime that is free from the effect of refraction defocusing, with a divergence of only 0.5–0.6 mrad. The discharge plasma is produced in capillary channels with length of 45 cm, where the Fresnel number of the gain medium is of the order of unity. The full laser energy is about 300 μJ. The spatial coherence of the laser has been experimentally investigated using a Young's double-slit interferometer and analyzed assuming a Gaussian Schell-model source and the generalized Van Cittert–Zernike theorem. We demonstrate the achievement of almost full spatial coherence and a near-Gaussian intensity distribution.

DOI: 10.1103/PhysRevA.70.023818 PACS number(s): 42.55.Vc, 42.25.Kb, 42.60.Jf

I. INTRODUCTION

The interest in many kinds of applications, ranging from soft-x-ray interferometry, microscopy, and x-ray holography [1] has strongly motivated, in the last few years, the development and improvement of soft-x-ray lasers (XRLs) (see, for example, the review papers [2–4]). Among the different x-ray sources actually available, XRLs have the highest peak spectral brightness, a very large energy per pulse, and could be developed in the near future as tabletop devices [5–7]. However, the requirements for mirrorless amplification and high-density gradients in the plasma active medium of XRLs make it difficult to control the amplification of the x-ray radiation and to produce highly collimated beams with the high spatial coherence required for the applications [8–16]. In this regard, several interesting experimental investigations have been performed with conventional XRLs created in laser-produced plasmas. Among other results, a highly collimated laser beam at 18.9 nm has been obtained [17,18] in slab molybdenum targets through a longitudinally pumped transient collisional excitation x-ray laser, and more recently [18] a totally coherent 0.2-mrad x-ray beam has been demonstrated at 13.9 nm using the separate excitation of a laser oscillator and an amplifier [18]. Unfortunately, the high collimation of the beam [17,18] and the full spatial coherence [18] achieved in these experiments is obtained at the expense of the XRL energy (<1 μJ), which is here much too low to be of practical interest. Substantial progress in the production of XRLs with characteristics useful for applications has been obtained in recent years by Rocca *et al.* [5] with a pumping scheme based on fast capillary discharge (FCD). The use of FCDs has allowed the effective excitation of a 46.9-nm line in Ne-like Ar with the achievement of high energy per pulse and a high repetition rate in an extremely compact experimental device. In [19,20] almost full spatial coherence of the 46.9-nm laser beam with millijoule energy per pulse in 36-cm-long discharge plasmas was recently demonstrated. In agreement with numerous theoretical analyses [21,22], in Ref. [20] the high spatial coherence is obtained by strong refraction defocusing. The refraction provides that the coherence length scales much faster than linearly with the length of the plasma. An effect of the refraction is also the production of an annular distribution of the laser intensity with a divergence of 4–5 mrad [19,20]. Detailed investigations of the FCD technique have led to a further improvement of the 46.9-nm laser in terms of divergence and distribution of intensity [23]. In Ref. [23] Ritucci *et al.* reported on a saturated 46.9-nm capillary discharge laser with a submilliradiant divergence, produced in a regime of amplification free from the effect of refraction defocusing. In this paper we present results obtained in measurements of the spatial coherence of this 46.9-nm capillary discharge laser characterized by a high collimation. The laser beam is produced in capillary channels having lengths up to 45 cm. In this condition the laser divergence reaches the value of 0.5–0.6 mrad. We experimentally demonstrate the almost full spatial coherence of this beam and the near-diffraction-limited divergence.

II. EXPERIMENTAL METHOD

The capillary discharge laser at 46.9 nm is obtained by the collisional excitation of the $3p$-$3s$ transition of Ne-like Ar [see Fig. 1(a)]. The hot and high-density Ar plasma column, suitable for laser amplification on the $3p$-$3s$ transition, is produced by discharging a fast current pulse with amplitude of 20–24 kA and half-cycle duration of 150–180 ns through a 3-mm-diameter alumina capillary channel initially filled with pure Ar gas [24]. The plasma formed in the discharge is heated by the z-pinch compression of the plasma along the capillary axis. The plasma compression is induced by the magnetic force created by the current itself. The plasma temperature (≈ 50–80 eV) and density $[(3-4)\times 10^{18}\ \mathrm{cm}^{-3}]$ required for the population inversion are reached close to the final stage of the compression when the plasma diameter has reached a value in the range of 250–300 μm [2]. As the amplification takes place in a single-pass regime, the Fresnel number of the gain medium $F = ka^2/L$ should be lower than unity to produce a full spatial coherence [25] (a and L are the radius and the length of the gain medium, respectively, and k is the free-space wave number). Since this condition requires

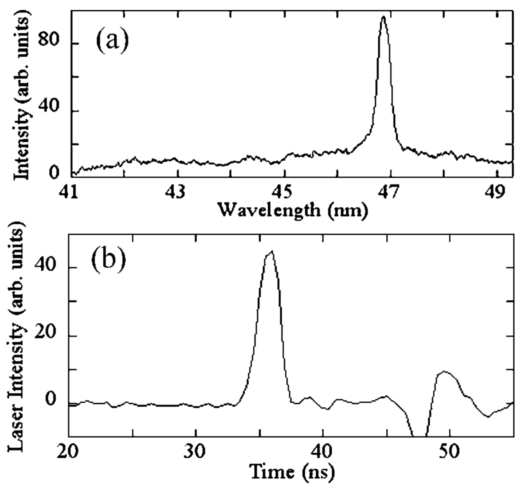

FIG. 1. (a) Lineout of a typical spectrum obtained between 41 and 49 nm, showing the dominating laser line at 46.9 nm, and (b) time evolution of the saturated laser emission produced in 45-cm-long capillary discharges.

a plasma length $L > ka^2$ we have increased the length of the capillary channels up to 45 cm, which is sensibly longer than that used in previously reported experiments [19,20]. The discharge is driven by a tabletop power supply system composed of a Marx generator and a 10-nF water dielectric capacitor. This device can operate at the maximum pulse repetition rate of 0.2 Hz. The capillary channel is initially filled by pure Ar gas at low pressure between 0.3 and 0.5 Torr. A low-amplitude current pulse of 20 A and duration longer than several microseconds crosses the capillary tube before the 20–24 kA discharge current (main discharge) is fired. The 20-A current pulse just preionizes the Ar and creates suitable initial conditions for a uniform plasma z pinch. It should be noted that no lasing effect has been obtained without the use of this preionization current pulse. By contrast, using preionization, a strong laser emission is produced about 35 ns after the starting of the main discharge and it has duration at full width at half maximum (FWHM) of 1.7 ns [see Fig. 1(b)]. The intensity distribution of the beam is analyzed by an imaging detector composed of a phosphor screen and a charge-coupled device camera with 1392×1040 pixels and 4.65-μm pixel size. At a capillary length of 16 cm the laser amplification achieves gain saturation [26]. Moreover, in the highly saturated regime, with the active medium longer than 20 cm, the 46.9 nm laser line becomes so intense as to strongly dominate the uv and soft-x-ray spontaneous radiation emitted by the plasma. At 45 cm the laser intensity at the capillary output reaches the value of $\approx 8 \times 10^8$ W/cm^2, which is about 20 times the saturation intensity [26] (Fig. 1).

III. EXPERIMENTAL RESULTS AND ANALYSIS

The intensity distribution of the laser beam is sensitive to the initial discharge conditions [23]. In particular, using the long excitation current pulses with duration of 170–180 ns and an initial gas pressure in the range of 0.43–0.48 Torr we find a beam structure dominated by an axially peaked and highly collimated radiation. Figures 2(a) and (b) show the typical far-field pattern obtained in this range of pressure by using a capillary channel of 45 cm and the corresponding plot profile. The far-field measurements have been performed by placing the imaging detector on the beam axis at a distance of 210 cm from the capillary output. The central peak observed in Fig. 2 and obtained using 45-cm-long capillaries has a FWHM divergence of only 0.6 mrad. We verified, over hundreds of laser shots, a quite good reproducibility of this beam structure and observed that this profile optimizes the energy extracted by the plasma medium to the average value of 300 μJ. In our experimental conditions, the central component constitutes the dominant part of the laser emission as it contains almost 70% of the full energy of the laser. The large annular pedestal, which can be observed in Fig. 2 around the central peak, has a full divergence of 5 mrad and intensity about five times smaller than that of the central peak. From Fig. 2(b) one can see that the intensity distribution of the central component can be reasonably approximated to a near-Gaussian distribution. This regime of operation is quite different from that reported in previous characterizations of a 46.9 nm capillary discharge laser

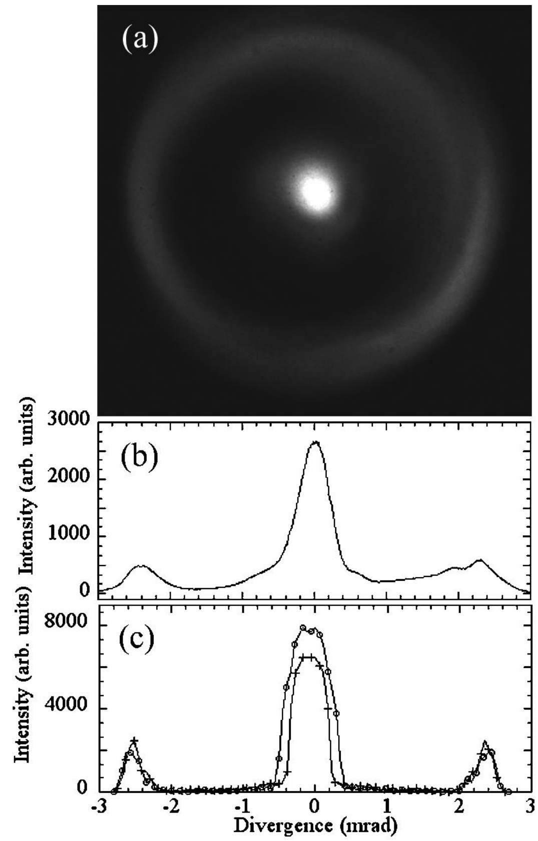

FIG. 2. (a) Typical far-field laser beam structure produced in 45-cm-long plasmas using an initial gas pressure between 0.43 and 0.48 Torr and (b) the corresponding lineout. (c) Theoretical far-field intensity profiles calculated by the ray-tracing code with a quartic distribution of the electron density obtained using $N_0 = 3 \times 10^{18}$ cm^{-3} and $R = 160$ μm. $\Delta N = 4 \times 10^{16}$ (solid line with crosses) and 1×10^{17} cm^{-3} (solid line with with open circles).

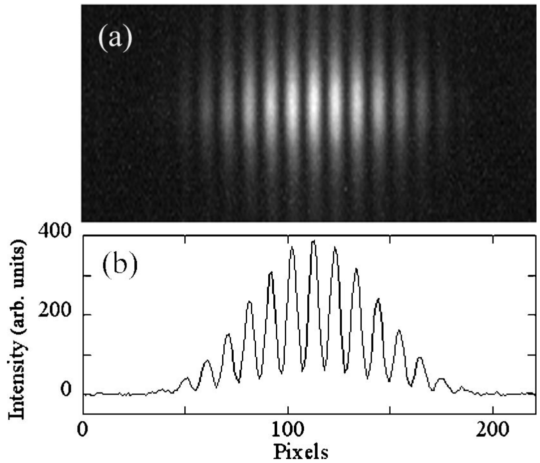

FIG. 3. (a) Diffraction fringe pattern produced by central component of the 46.9-nm laser beam on two 30-μm-wide slits with a separation of 130 μm placed at 42 cm from the capillary output and (b) the corresponding lineout.

[19,20], where, as the amplification is dominated by strong refraction defocusing, the beam has only the characteristic annular shape with a peak-to-peak divergence of 5 mrad. The generation of a laser beam with a submilliradiant divergence and a near-Gaussian intensity distribution can be of quite practical importance for the development of applications.

To study the transverse coherence of this submilliradiant and axially centered emission, we have performed experiments based on classical Young's double-slit interferometry. In this kind of experiment, provided the slits are illuminated with the same intensity, the modulus of the coherence degree $|\mu_{12}|$ is equal to the fringe visibility $V=(I_{\max}-I_{\min})/(I_{\max}+I_{\min})$. Different slit separations have been used for the measurement: two pairs of 30-μm-wide slits with a slit separation Δx of 90 μm and 130 μm, respectively. The slits were placed at a distance of 42 cm from the capillary output and the phosphor screen at 170 cm from the slits. At a distance of 42 cm the full width of the beam at half maximum, measured by use of fluorescent LiF films [26,27], previously positioned on the plane of the slits, resulted in 290 μm. Figure 3(a) shows a typical single-shot interferogram obtained using slits with a separation of 130 μm and produced by the only contribution of the central peak. In these conditions we found an excellent fringe visibility (≈ 0.78) as demonstrated in the corresponding lineout [Fig. 3(b)]. Figure 4 shows the experimental decrease of the coherence degree from 0.9 to 0.78

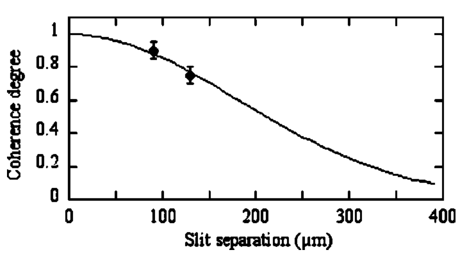

FIG. 4. Measured degree of the spatial coherence $|\mu_{12}|$ versus the slit separation (dots). The solid line represents the best fit of $|\mu_{12}|$ obtained using a Gaussian profile. L_c results as 190 μm.

with increase of the slit separation from 90 to 130 μm.

These experimental data have been analyzed by treating the laser as a planar Gaussian-Schell model source [28]. This approach has been proved to be particularly suitable for the description of the coherence properties of multimode laser sources. Within the framework of this model the intensity profile of the source and the degree of transverse coherence both have Gaussian distributions. The coherence length L_c is determined from the behavior of $|\mu_{12}|$ versus the slit separation Δx according to the relation $\mu_{12}=\exp(-\Delta x^2/2L_c^2)$. The value of L_c is determined by the distance at which the value of μ_{12} is reduced to $1/\sqrt{e}$ [28]. By fitting the experimental behavior of $\mu_{12}(\Delta x)$ (see Fig. 4) with a Gaussian profile (with $|\mu_{12}|=1$ at $\Delta x=0$) and taking into account the experimental inaccuracy of the measurements, we found at the distance of 42 cm a transverse coherence length of 190 ± 10 μm.

To determine the characteristics of the equivalent Gaussian-Schell model source, such as its dimensions and the intrinsic coherence length, we have used the generalized Van Cittert–Zernike theorem [28] (one can also see, as an example, the application of this theorem to the analysis of an ASE laser source in [29]). As discussed in [28], the total transverse coherence length $L_c(z)$ at any transverse cross section of the beam is the sum of a contribution σ_g, which is the coherence length at the plane of the source (the intrinsic coherence length), and a contribution $L_p(z)$ coming from simple propagation in free space [28]:

$$L_c(z) = \sqrt{\sigma_g^2 + L_p^2(z)}. \tag{1}$$

The intrinsic and acquired coherence lengths are determined by the equations

$$L_p(z) = \frac{z\lambda}{4\pi}\frac{\sigma_g}{\sigma_S}\left(\frac{1}{4\sigma_S^2} + \frac{1}{\sigma_g^2}\right), \tag{2}$$

$$\theta = \frac{\lambda}{4\pi\sigma_S}\left(4 + \frac{\sigma_g}{\sigma_S}\right), \tag{3}$$

where θ is the far-field beam divergence, σ_S the source radius, and z the distance between the source and the diffraction plane. In Eq. (3) we consider as the beam divergence the angle measured with respect to the beam axis at which the intensity reduces to $1/\sqrt{e}$. The exact location z of the equivalent planar Gaussian-Schell source with respect to the diffracting plane has been determined by recording the interference patterns produced by the diffraction of the laser radiation on a blade edge obstacle. Comparing the experimental distances between the fringes in the interference pattern with the distances calculated by the Huygens-Fresnel integral, we found that the equivalent Gaussian-Schell source is located inside the plasma column at ≈ 22 cm from the output end of the capillary tube, that is, approximately in the middle of the active medium. From Eqs. (1)–(3), we calculate a value of $L_p \approx 188$ μm, a value of $\sigma_g \approx 30$ μm, and a value of $\sigma_S \approx 28$ μm, with an estimated accuracy of ±8%. As the intrinsic transverse coherence length is approximately equal to the source dimension, the laser beam can be considered almost fully coherent. The number of modes sustained by the active medium can be estimated by the relation $N = \sigma_S^2/\sigma_g^2 \approx 1$. This value of N indicates that the laser operates using essentially the lowest-order transverse modes. The beam quality factor of the laser [29], $M^2 = \sqrt{1+\sigma_S^2/\sigma_g^2} \approx 2$ provides evidence of the quasi-Gaussian feature of the collimated laser radiation.

Because of the mirrorless amplification, the properties of divergence and coherence of a soft-x-ray laser is strongly related to the typology of the electron density and gain profiles in the plasma medium. In our case, we can attribute the formation of the low-divergence beam to the presence, at the moment of lasing, of a region, close to the plasma axis, with a rather flat plateau in the electron density distribution. In a z-pinch capillary discharge, this particular configuration, in which the refraction can be almost totally negligible close to the plasma axis, can be formed, during the compression, before the plasma has collapsed on the axis. The achievement of the gain before the final collapse can be attributed to the effect of the slow excitation current pulse. The features of the spatial distribution of the electron density at the moment of lasing can be estimated simulating the experimental intensity distribution of the laser by a ray-tracing code based on the standard eikonal equation in paraxial approximation

$$\frac{d^2r}{dz^2} = \frac{d\ln(\eta)}{dr} \tag{4}$$

and on the equation

$$\frac{dI}{ds} = \frac{g(s)I(s)}{1 + I/I_{\text{sat}}} \tag{5}$$

for the calculation of the ray intensities. Equation (5) takes into account the saturation of the gain at the laser intensity $I = I_{\text{sat}}$. In the simulations, different hypotheses for both the electron density distribution and the gain profile should be considered. For the gain we have assumed a paraboliclike distribution $g(r) = g_0(1 - r^2/a^2)$ with an on-axis maximum g_0 of 1 cm^{-1} and a radius of 150 μm. This distribution has been chosen according to previous theoretical analysis of the plasma dynamics of the 46.9-nm capillary discharge laser [30]. To shape the low-refraction region we have assumed a quarticlike curve for the density distribution, $N_e(r) = -(N_0/R^4)r^4 + (2\sqrt{N_0 \Delta N}/R^2)r^2 + N_0$ where R is the plasma radius and N_0 is the on-axis value of the electron density. The on-axis depression ΔN in the quartic curve is chosen to be much less than N_0. The gain and the density profiles are both set to be zero for $|r| > a$ and $|r| > R$, respectively. Despite the approximations of the model and of the gain and density profiles used, we found a very good agreement between the experimental and theoretical intensity distributions [see Fig. 2(c)] considering for N_0 the value of 3×10^{18} cm^{-3}, for R the value of 150 μm, and for ΔN the value of $\approx 4 \times 10^{16}$ cm^{-3}. From the parameters derived from the fitting we can estimate that the diameter of the low-refraction region is about 90 μm, which is approximately three times smaller that the full dimensions of the gain region. From the simulations we find that the collimated radiation is entirely formed inside this low-refraction region. This effect is well illustrated in the map of Fig. 5, which reports the distribution of the ray trajectories inside the plasma column, taking into account the quartic profile of the electron density. The rays generated inside the 90-μm region close to the plasma axis with emission angle smaller than the acceptance semiangle of 0.3 mrad can be amplified efficiently, remaining close to the plasma axis through the whole propagation. On the contrary, the large number of rays that are emitted with angle greater than about 0.3 mrad and/or are produced outside this narrow rod are affected by strong refraction defocusing. The small dimensions of the low-refraction area and the length of the plasma column provide for the active medium a value of the Fresnel number F of ≈ 1.5. The number of modes estimated from this value of F ($N \approx F^2$) is in good agreement with the low number of supported modes found by experimental analysis of the beam coherence. The results of this investigation show that in our experiment an almost fully coherent beam with high collimation is created in the absence of refraction through the reduction of the transverse dimensions a of the plasma region, where the beam is efficiently amplified and, at the same time, through the increase of the length of the plasma column. The measured divergence and full spatial coherence have allowed us to estimate a coherent peak spectral brightness of the order of B_{coh} of $\approx 5 \times 10^{24}$ photons/s mm^2 mrad^2 within 0.01% spectral bandwidth, which represents one of the highest value obtained to date in a tabletop device.

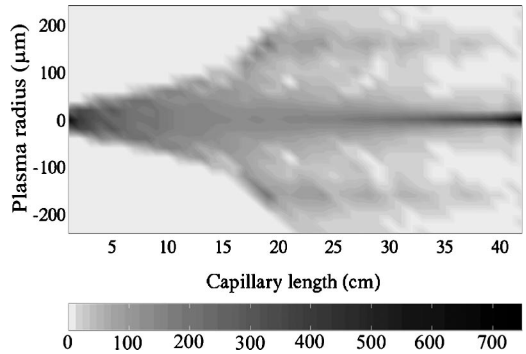

FIG. 5. Calculated map of the ray trajectories inside the plasma column obtained with the quartic profile of the electron density with $N_0 = 3 \times 10^{18}$ cm^{-3}, $\Delta N = 4 \times 10^{16}$ cm^{-3}, and $R = 160$ μm.

IV. CONCLUSIONS

In conclusion, we have reported on the experimental investigation of the transverse coherence of a highly collimated 46.9-nm soft-x-ray beam with a near-Gaussian profile produced in a capillary discharge plasma. The laser is operating in a highly saturated regime. By a classical double-slit interferometry and the generalized Van Cittert–Zernike theorem, we have demonstrated the almost full spatial coherence of the beam. High coherence is obtained in a regime that is free from the effect of refraction defocusing and by the use of elongated plasma columns with length up to 45 cm. In the collimated beam structure the laser demonstrates a substantial large energy of ≈ 200 μJ and a peak spectral brightness of $\approx 5 \times 10^{24}$ photons/s mm^2 mrad^2 within 0.01% spectral bandwidth.

We believe that the presented results give insight into the physics of generation of nearly coherent soft-x-ray laser beams with nearly diffraction-limited divergence. In particular, they help to understand the mechanism of formation of the submilliradiant, nearly Gaussian x-ray laser beams excited in refraction-gradient and extremely long capillary *z*-pinch plasmas. These results represent a method for further improvement of the characteristics of this kind of laser.

ACKNOWLEDGMENTS

This work was supported by the Italian National Institute of Nuclear Physics. We want to acknowledge Professor S. V. Kukhlevsky, Dr. A. Faenoy, and Dr. T. Pikuz for their help and useful discussions. The authors are also grateful for the kindness of Dr. R. Tomassini for having supported us with the double slits.

[1] D. Attwood, *Soft X-Rays and Extreme Ultraviolet Radiation* (Cambridge University Press, New York, 1999).
[2] J. Rocca, Rev. Sci. Instrum. **70**, 3799 (1999).
[3] H. Daido, Rep. Prog. Phys. **65**, 1513 (2002).
[4] G. J. Tallents, J. Phys. D **36**, R259 (2003).
[5] J. Rocca, V. Shlyaptev, F. Tomasel, O. Cortazar, D. Hartshorn, and J. Chilla, Phys. Rev. Lett. **73**, 2192 (1994).
[6] P. Nickles, V. Shlyaptev, M. Kalachnikov, M. Schnurer, I. Will, and W. Sandner, Phys. Rev. Lett. **78**, 2748 (1997).
[7] J. Dunn, Y. Li, A. Osterheld, J. Nilsen, J. Hunter, and V. Shlyaptev, Phys. Rev. Lett. **84**, 4834 (2000).
[8] J. E. Trebes *et al.*, Phys. Rev. Lett. **68**, 588 (1992).
[9] R. E. Burge *et al.*, J. Opt. Soc. Am. B **15**, 2515 (1998).
[10] B. Rus, T. Mocek, A. R. Prag, M. Kozlova, D. J. D. P. G. Jamelot, A. Carillon, and D. Ros, Phys. Rev. A **66**, 063806 (2002).
[11] J. Zhang *et al.*, Phys. Rev. A **54**, R4653 (1996).
[12] R. Kodama, D. Neely, Y. Kato, H. Daido, K. Murai, G. Yuan, A. MacPhee, and C. Lewis, Phys. Rev. Lett. **73**, 3215 (1994).
[13] A. Carillon *et al.*, Phys. Rev. Lett. **68**, 2917 (1992).
[14] J. Nilsen, J.C. Moreno, L. B. DaSilva, and T. W. Barbee, Jr., Phys. Rev. A **55**, 827 (1997).
[15] P. Lu, E. Fill, Y. Li, J. Maruhn, and G. Pretzler, Phys. Rev. A **58**, 628 (1998).
[16] D. Benredjem, J. Kuba, C. Moller, and O. Zabaydullin, Phys. Rev. A **67**, 043816 (2003).
[17] T. Ozaki, R. Ganeev, A. Ishikawa, T. Kanai, and H. Kuroda, Phys. Rev. Lett. **89**, 253902 (2002).
[18] M. Nishikino, M. Tanaka, K. Nagashima, M. Kishimoto, M. Kado, and T. Kawachi, Phys. Rev. A **68**, 061802 (2003).
[19] C. Macchietto, B. Benware, and J. Rocca, Opt. Lett. **24**, 1115 (1999).
[20] Y. Liu, M. Seminario, F. G. Tomasel, C. Chang, J. Rocca, and D. Attwood, Phys. Rev. A **63**, 033802 (2001).
[21] R. A. London, M. Strauss, and M. Rosen, Phys. Rev. Lett. **65**, 563 (1990).
[22] P. Amendt, R. London, and M. Strauss, Phys. Rev. A **47**, 4348 (1992).
[23] A. Ritucci *et al.*, Europhys. Lett. **63**, 694 (2003).
[24] G. Tomassetti *et al.*, Eur. Phys. J. D **19**, 73 (2002).
[25] A. Siegman, *Lasers* (University Science Books, Sausalito, CA, 1999).
[26] G. Tomassetti *et al.*, Opt. Commun. **231**, 403 (2004).
[27] G. Tomassetti *et al.*, Europhys. Lett. **63**, 681 (2003).
[28] L. Mandel and E. Wolf, *Optical Coherence and Quantum Optics* (Cambridge University Press, New York, 1995).
[29] R. Tomassini, S. Insam, and E. Fill, Opt. Commun. **180**, 277 (2000).
[30] C.H. Moreno, M.C. Marconi, V.N. Shlyaptsev, B.R. Benware, C.D. Macchietto, J.L.A. Chilla, J.J. Rocca, and A.L. Osterheld, Phys. Rev. A **58**, 1509 (1998).